PHOTOPHYSICS OF SOME COMMON FLUORESCENCE STANDARDS

STEPHEN R. MEECH and DAVID PHILLIPS
The Royal Institution, 21 Albemarle Street, London W1X 4BS (Gt. Britain)
(Received April 12, 1983)

Summary

An accurate study of the fluorescence decay and fluorescence quantum yield of three fluorescence standards is made. From data on 9,10-diphenylanthracene it is concluded that (a) the refractive index squared correction employed in relative quantum yield measurements in right-angle fluorometers is valid, (b) a refractive index squared term is required for the valid comparison of radiative lifetimes of the same molecule measured in different solvents and (c) the fluorescence quantum yield is less than unity and is essentially independent of the solvent ($\phi_F = 0.93 \pm 0.03$ in four non-polar solvents).

Further results are presented on the complex kinetics of the fluorescence decay of quinine bisulphate in aqueous H_2SO_4 solutions; a model is proposed which accounts adequately for these observations. Some results are presented for 2-aminopyridine in aqueous H_2SO_4 solutions which suggest that this may also be a useful fluorescence standard; we measured $\phi_F = 0.66$ and $\tau_F = 9.6$ ns in both 1 and 0.1 N H_2SO_4 solutions. However, disagreement about these values and the strong temperature dependence of ϕ_F that is observed renders this compound less acceptable as a standard than quinine bisulphate in 1 N H_2SO_4 solution.

1. Introduction

Time-resolved and steady state fluorescence spectroscopy has assumed an increased importance in recent years in subjects as diverse as biological membrane studies [1], polymer [2] and protein dynamics [1], and solar energy conversion [3]. These studies are in addition to the more fundamental interest in electronic spectroscopy and fast relaxation processes in solution etc. The advent of laser technology has permitted many advances in the area of time-resolved fluorescence [4], but it remains true that a more detailed understanding of molecular electronic states requires a knowledge of the fluorescence (or phosphorescence) quantum yield. The accurate measurement of luminescence quantum yields is a notoriously difficult problem, as has been noted in several excellent reviews [5 - 7].

0047-2670/83/$3.00

The major aims of the current work are (1) to apply sophisticated time-resolved fluorescence techniques to a study of three quantum yield standards and to demonstrate how such measurements may add to the reliability of quantum yield determinations, and (2) to describe and calibrate an integrating sphere spectrofluorometer and to restate some of the techniques that are essential in the accurate determination of ϕ_F. Thus a study of the quantum yield and decay time(s) of three standards that are commonly used in fluorescence spectroscopy is presented. The standards investigated are 9,10-diphenylanthracene (DPA) in a variety of non-polar solvents, quinine bisulphate (QBS) in H_2SO_4 solutions and 2-aminopyridine (2AP), also in H_2SO_4 solutions.

Our subsidiary aims in this study are (a) to determine what refractive index correction is required for the radiative lifetime of a molecule in solution (the theoretical refractive index correction) since this is important when data for the same molecule in various solvents are to be compared and high accuracy is required, (b) to determine experimentally the appropriate geometrical refractive index correction, to ensure that the value of n^2 determined for several geometries is experimentally valid, (c) to study further the previously reported [8] complex decay kinetics of QBS and (d) to discuss the photophysics of 2AP in H_2SO_4 solutions since this may be an alternative standard to QBS (see below).

There are two classes of quantum yield measurement. The absolute method described by Vavilov [9] and others [10, 11] is really restricted to samples of high quantum yield, as are other absolute methods such as chemical actinometry [12].

The most common method of quantum yield determination, the relative method, is described here. This method simply involves the comparison of the corrected areas of the fluorescence spectra of a standard and a sample. The area A is given by $A = \phi_F OD$, where OD is the optical density of the sample. Thus the yield is determined from

$$\phi_F = \frac{A}{A^{(1)}} \frac{(OD)^{(1)}}{OD} \phi_F^{(1)} \tag{1}$$

if it is assumed that the two spectra are measured under the same conditions. The superscript refers to a standard parameter. Unfortunately all the parameters required are subject to non-random distortions (see below and ref. 5). In the light of these difficulties Demas and Crosby [5] recommended the following minimum amount of information that is required to assess the validity of the measurement: the technique employed; the yield assumed for the standard; the excitation wavelength; the method of data reduction; the technique used for the absorption measurements; the instrumentation; the experimental geometry; the monochromator bandpasses; the spectral correction technique used and the correction curve derived from it; the stray light characteristics of the instrument and any subsequent correction procedure; the refractive index correction applied, if any; the extent of reabsorption

and re-emission effects; sample preparation methods; errors in the measurements, both calculated and subjectively estimated; the presentation of the values obtained for samples of known quantum yield.

2. Experimental details

The fluorescence lifetimes reported here were measured using the time-correlated single-photon counting technique, the excitation source being a Spectra Physics synchronously pumped cavity-dumped dye laser. This system, and in particular the data reduction techniques employed which give increased confidence in the decay kinetics that are determined, has been described elsewhere [13].

The quantum yields were determined using a home-built fully corrected integrating sphere spectrofluorometer. In this instrument the sample is excited at the centre of a sphere, the inside of which has been coated with a high reflectance material ($BaSO_4$ in this case). The emission is collected through a port which views only the scattering surface. Thus all the radiation collected has undergone at least one interaction with the surface, and since it has no "memory" of its original direction no geometrical refractive index correction is required. This correction arises in a conventional fluorometer because the different refractive indices of the sample and the standard result in the detection system "seeing" different fractions of the emitted luminescence. This was first discussed by Hermans and Levinson [14], who proposed an n^2 (n is the refractive index) correction for right-angle viewing geometry. This has recently been questioned [15], but careful calculations [16, 17] demonstrate that n^2 is theoretically valid for a number of experimental geometries. This has not been tested experimentally, and therefore is one of the aims of this study.

An integrating sphere has some other advantages. The spatial inner filter effect, which may distort measurements in conventional instruments when $OD \neq (OD)^{(1)}$ because the detector may preferentially collect radiation from a particular point in the sample, is suppressed by the arrangement of the collecting optics of an integrating sphere. Conversely the inner filter effect due to reabsorption of radiation may be amplified in an integrating sphere, where the fluorescence may make multiple passes through the sample prior to detection. It is easy to ensure that this does not distort the measured spectra by simply recording the emission spectrum, as a function of sample concentration, of a fluorophore that has a significant overlap of the absorption and fluorescence spectra. We chose anthracene and DPA and found that the fluorescence spectra were invariant with concentration below an OD_{max} of 0.07; this was adopted as the upper OD limit for our measurements. One further advantage of an integrating sphere is that the scattering process randomizes the polarization of the emitted luminescence; thus the polarization-dependent sensitivity of the collection system is not a problem.

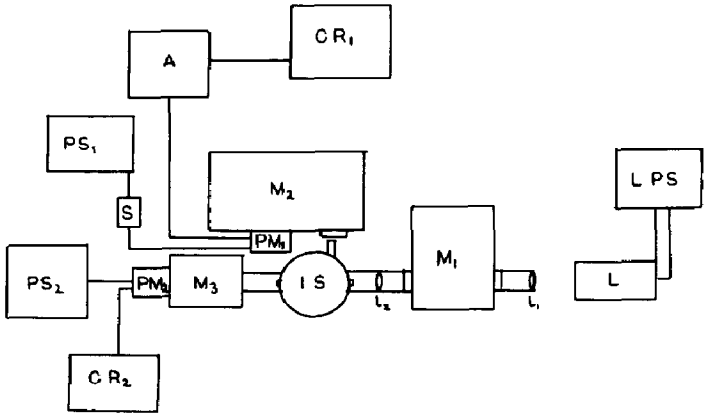

Fig. 1. Block diagram of the integrating sphere spectrofluorometer: LPS, lamp power supply; L, 450 W xenon lamp; M_1, M_2, M_3, monochromators; IS, integrating sphere; PS_1, PS_2, power supplies; PM_1, PM_2, photomultiplier tubes; A, picoammeter; CR_1, CR_2, chart recorders; l_1, l_2, lenses; S, stabilizer.

Consequently, the integrating sphere spectrofluorometer is ideal for measuring the luminescence from slowly rotating macromolecules.

The integrating sphere–spectrofluorometer was constructed as shown in Fig. 1. The inside of the sphere, which was 20 cm in diameter, was evenly coated with a 100% reflectance $BaSO_4$ paint obtained from Eastman–Kodak. A block diagram of the instrument is given in Fig. 1.

The light source was a 450 W xenon lamp powered by a home-built stabilized power supply. The light from this was focused onto the entrance slit of a Rank Precision D330 monochromator; the slit height was reduced to about 3 mm such that it was completely filled by the focused beam. The height of the exit slit was similarly reduced. The emerging monochromatic light was further focused by a long focal length lens to a waist at the centre of the integrating sphere.

The beam emerging from the sphere passed onto the entrance of a Bausch and Lomb high intensity monochromator, the output of which impinged directly onto the photocathode of a 1P28 phototube.

This monochromator–photomultiplier combination was intended for use in transmission intensity measurements. In fact, for the quite low optical density samples used in these experiments, a number of difficulties were associated with such a technique. This part of the instrument was only used for some calibration measurements (see below).

The fluorescence emission was routed directly into a double D331 Rank Precision monochromator. The fluorescence intensity was measured using an R928 Hammamatsu photomultiplier tube. The photocurrent from the R928 was routed to a Victoreen electrometer and the output from this was recorded on a Tekman chart recorder.

The fluorescence spectra were fully corrected for the wavelength dependence of the detection system, the correction curves being obtained by the quantum counter–scatterer method [18]. The only difference between

our method and those reported in the literature is that the correction curves were recorded with the integrating sphere in place and thus any wavelength dependence of the scattering efficiency of $BaSO_4$ is included in them. The quantum counter used for excitation wavelengths above 350 nm was rhodamine B (RB) in ethylene glycol at a concentration of 8 g l^{-1}; at wavelengths below 350 nm QBS in 1 N H_2SO_4 at a concentration of 4 g l^{-1} was used. We find, with Melhuish [18], that RB is not a good quantum counter below 350 nm (see below). The scatterer employed was a layer of MgO 1 mm thick on quartz [19]. We used the curves generated in this way to correct our measured fluorescence spectra of QBS and 2AP. The agreement with published spectra [19] was excellent [20].

One serious problem in the relative determination of ϕ_F is that the measured OD may not accurately reflect the amount of light absorbed by the fluorophore. This may arise because of the different characteristics of the monochromators of the instruments used for the absorption measurement and in the excitation system. This point, which is most important for samples with a structured absorption spectrum, is frequently disregarded in determinations of ϕ_F. Since we found that use of the intensity monitor (Fig. 1), which would have directly recorded the amount of light absorbed by the sample, led to unacceptably large errors in our system, we have instead calibrated a PE 554 spectrophotometer in the following manner (the PE 554 has the additional desirable feature of permitting an accurate background correction). The ODs of various concentrations of anthracene were determined in both the PE 554 and the integrating sphere (employing the intensity monitor); when they were plotted against one another a slope of unity was found. We similarly measured the OD of QBS at different concentrations in the PE 554 and plotted these against the fluorescence intensity measured in the integrating sphere; again the slope was unity. QBS in H_2SO_4 is not an ideal sample for this test since its absorption is unstructured, but it has the advantage that it does not exhibit extensive self-quenching [21]. We conclude that the PE 554 accurately determines the amount of light absorbed by the sample in the fluorometer, provided that the resolution of each instrument is the same.

Monochromator wavelength calibrations were checked using low pressure mercury lamps and standard spectra. The possibility of errors arising from a variation in the lamp intensity between the measurement of the sample and of the standard spectra was eliminated by employing the method of Parker and Rees [6].

For all the quantum yields reported here at least two (and usually more) sample concentrations were employed, each sample being excited at at least two wavelengths. The errors were calculated using the method given in ref. 10. Our subjective estimate of the accuracy of these determinations is "better than 5%".

For all measurements reported here the standard used was an undegassed solution of QBS in 1 N H_2SO_4. The value of ϕ_F is 0.546 [21]. This value has been checked by numerous absolute measurements [11, 21, 22]. The excitation and emission bandpasses were 2 nm and 3 nm respectively.

Cyclohexane (BDH, fluorometric grade) was passed through a silica-on-alumina column. The hexane (mixture) (Aldrich gold label) was fractionally distilled. Decalin (Aldrich (a mixture of isomers)) was purified by vacuum distillation. Benzene (Aldrich gold label) was used as received. The water was triply distilled, and the H_2SO_4 was BDH Aristar grade. All solvents were non-fluorescent when excited at the appropriate wavelengths on an MPF-4 spectrofluorometer set for maximum sensitivity.

QBS was recrystallized three times from water, 2AP (Aldrich gold label) was recrystallized twice from cyclohexane and DPA was scintillation grade and was used without further purification.

3. Results and discussion

3.1. Calibration

For the purpose of calibration of the instrument the quantum yields of several standard compounds should be measured. However, since one object of this paper is to test the validity of the n^2 correction, and many of the standard yields that have been measured have employed this correction, this would not be a valid procedure. Rather, a combination of quantum yield ϕ_F and fluorescence lifetime τ_F data has been employed. Measurements of τ_F are subject to far fewer distortions than are those of ϕ_F, provided that sufficient care is taken with them [13]. The results are presented in Tables 1 and 2.

Each quantum yield presented in Tables 1 and 2 was measured for at least three concentrations, with the exception of the undegassed DPA–cyclohexane sample for which two concentrations were used. Each concentration of solute was excited at at least two wavelengths. QBS in 1.0 N H_2SO_4 was the standard ($\phi_F = 0.546$). Each measurement was wholly independent of the others, except for the DPA samples; their spectra and lifetimes were measured before and after degassing.

The three ratios of lifetime and quantum yield measurements shown in Table 2 exhibit remarkably good agreement. We should note, however, that this may be fortuitous since the errors in the measured yields are larger than would be suggested from these results. However, we can conclude that the true values lie within the calculated error, and our estimated error of 5% or less is probably correct.

The agreement between the measured quantum yields and those available in the literature is quite good. The reduction in the quantum yield of QBS as the normality of the acid solution is reduced is very well documented, having been observed in at least one absolute measurement [11]. This agreement is encouraging. The yield of 2AP in 0.1 N H_2SO_4 has previously been measured relative to both QBS–1 N H_2SO_4 ($\phi_F = 0.546$ [23]) and DPA–cyclohexane ($\phi_F = 1.00$ [25]). There is a significant disagreement between the measured values. Our result lies between them. The yield of DPA has been a controversial subject for many years; published values lie between 0.84 and 1.12 [24].

The measurements will now be discussed in more detail.

TABLE 1

A comparison of the measured quantum yield with the measured lifetimes and some published quantum yield measurements

Sample	*Solvent*	ϕ_F [a]	ϕ_F *(literature)*	τ_F (ns)
QBS	1.0 N H_2SO_4	(0.546)	0.546 [21], 0.54 [20], 0.56 [22]	≈ 20.4[b]
QBS	0.1 N H_2SO_4	0.52 (0.02)	0.51 [22], 0.50 [20]	≈ 19.1[b]
2AP	1 N H_2SO_4	0.65 (0.04)	—	9.6
2AP	0.1 N H_2SO_4	0.66 (0.05)	0.6 [8], 0.73 [22]	9.6
DPA	Undegassed C_6H_{12}	0.70 (0.04)	0.77 [23]	5.85
DPA	Degassed C_6H_{12}	0.91 (0.02)	Various (see ref. 24)	7.7

[a]The second numbers in parentheses represent errors.
[b]Mean value of the major component (see text).

TABLE 2

Ratios of comparable quantum yields and lifetimes

Ratio	ϕ_F	τ_F
[QBS (1 N)]/[QBS (0.1 N)][a]	1.05	1.06
[DPA (CyH)]/[DPA (O_2, CyH)][b]	1.3	1.32
[2AP (1 N)]/[2AP (0.1 N)][a]	0.985	1.0

[a]The numbers in parentheses refer to acid normality.
[b]CyH, cyclohexane.

3.2. 9,10-diphenylanthracene in non-polar media

We have chosen DPA for the study of the refractive index effects on fluorescence since its high quantum yield and quite good solubility in a variety of solvents make it an ideal standard for this purpose. Also it does not display any anomalous solvent effects (see below).

As stated above, the geometrical n^2 correction has been the subject of recent discussions [15 - 17]. Other workers have also addressed this problem, and the data of Morris *et al.* [26] are of particular note here. These workers used a right-angle viewing fluorometer to study the refractive index dependence of the quantum yield and fluorescence lifetime of DPA. They demonstrated the following.

(a) The measured quantum yield was a function of the slit width (viewing geometry) on the emission side of a right-angle fluorometer when an n^2 correction was uniformly applied and the standard and sample were dissolved in solvents of quite different refractive indices. No slit width dependence was observed when the refractive indices of the sample and reference solutions were quite close.

(b) The quantum yield of DPA varied but the radiative lifetime remained constant in the different solvents used (as might reasonably be

TABLE 3

Published values of some fluorescence quantum yields of 9,10-diphenylanthracene in benzene or cyclohexane reported since 1974 with lifetimes when available[a]

Solvent	ϕ_F	τ_F (ns)	*Method*	*Reference*
Benzene	0.96 (0.82)[b]	7.34	Relative[c]	[26]
	0.88[d]	6.95	Relative[d]	[28]
Cyclohexane	1.00[d]	7.58	Relative[d]	[28]
	1.05	—	Relative[e]	[32]
	0.95 (0.86)[b]	7.58	Relative[c]	[26]
	0.90	—	Absolute[f]	[27]

[a]Quantum yields reported before 1974 are given in ref. 24.
[b]Without application of standard refractive index correction (see ref. 26).
[c]Standards, DPA–ethanol (0.96), anthracene–ethanol (0.27), QBS–1 N H_2SO_4 (0.55).
[d]Calculated from the ratio given by Birch and Imhof [28] by assuming that ϕ_F(DPA–cyclohexane) = 1.00. These workers give only the ratio DPA(cyclohexane)/DPA(benzene). Birch [29] has measured an optoacoustic signal from the DPA–cyclohexane system which suggests that ϕ_F is less than 1.0.
[e]QBS–1 N H_2SO_4 (0.546) determined using an integrating sphere.
[f]Employing laser excitation and chemical actinometry.

expected) provided that no geometrical refractive index correction was applied. Our results contradict this result, although we still obtain a constant radiative rate constant. This discrepancy is resolved when a theoretical n^2 correction is applied.

Some recent values of the measured quantum yield of DPA in benzene and cyclohexane are presented in Table 3; the mean value for both solvents is 0.96. An extensive list of the quantum yields of DPA, measured prior to 1974, is given in ref. 24, Table 1. Also shown in Table 3 are the fluorescence lifetimes reported together with the respective quantum yield measurements. The agreement between the values of τ_F is quite good. This re-emphasizes the importance of reporting measured fluorescence lifetimes, whenever possible, with quantum yield measurements. The presence of either reabsorption effects or impurity emissions will be revealed by the lifetime measurement.

The measured values of the quantum yield and fluorescence decay times of DPA in four non-polar solvents of varying refractive index are shown in Tables 4 and 5. In all cases the fit of the fluorescence decay to a single-exponential function is good. The value of the quantum yield in cyclohexane is slightly lower than that usually reported, and some 15% lower than the value given by Ware and Rothman [32] who used a method very similar to the one described here. Our value, however, is in good agreement with the most recent absolute determination (ϕ_F(DPA–cyclohexane) = 0.90) [26], which was performed using the recommended technique of chemical actinometry in conjunction with laser excitation. Further we find that the measured quantum yield of this system is independent of the excitation wavelength between 370 and 300 nm. (While this manuscript was in

TABLE 4

Fluorescence decay characteristics of 9,10-diphenylanthracene in non-polar solvents: kinetic data

Solvent	ϕ_F	τ_F
Hexane	0.90 (0.04)	7.98
Cyclohexane	0.91 (0.02)	7.68
Decalin	0.94 (0.06)	7.17
Benzene	0.955 (0.02)	7.14

TABLE 5

Fluorescence decay characteristics of 9,10-diphenylanthracene in non-polar solvents: spectral data

Solvent	ν_a^{max} ($\times 10^3$ cm^{-1})	ν_e^{max} ($\times 10^3$ cm^{-1})	$\nu_a^{max} - \nu_e^{max}$ ($\times 10^3$ cm^{-1})	$\langle \bar{\nu}_f^{-3} \rangle_{AV}$ ($\times 10^{-13}$ cm^{-3})
Hexane	25.494	23.529	1.965	0.800
Cyclohexane	25.380	23.419	1.961	0.814
Decalin	25.304	23.392	1.912	0.825
Benzene	25.241	23.256	1.985	0.834

preparation Hamai and Hirayama [27] published full details of their experiments. Our results concerning the yield of DPA in cyclohexane and the validity of the geometrical n^2 correction (see below), which were obtained by different procedures, are in good agreement with theirs.)

Table 4 also shows that there is a small increase in the value of ϕ_F on going from a cyclohexane to a benzene solvent, which is in contrast with the decrease reported in previous work [28]. In fact the values which we obtained in all non-polar solvents are independent of the solvent within the limits of experimental error, the mean value being 0.93. A similar result was obtained in ref. 26 when an n^2 geometrical refractive index correction was applied.

A good internal test for the accuracy of this result should lie in a study of the behaviour of the radiative lifetime τ_R of DPA in various solvents, where

$$\tau_R = \frac{\tau_F}{\phi_F} = \frac{1}{K_F} \tag{2}$$

However, in calculating τ_R we must be aware of the possible influences of the medium. These can best be illustrated by considering the equation due to Strickler and Berg [33], as modified by Birks and Dyson [34], which relates the absorption intensity of a molecule to its radiative lifetime:

$$K_F = \frac{1}{\tau_R} = 2.880 \times 10^{-9} \frac{n_f^3}{n_a} \langle \bar{\nu}_f^{-3} \rangle_{AV}^{-1} \int \frac{\epsilon(\nu)\, d\nu}{\nu} \tag{3}$$

where

$$\langle \bar{\nu}_f^{-3} \rangle_{AV}^{-1} = \frac{\int I(\nu)\, d\nu}{\int \nu^{-3} I(\nu)\, d\nu} \tag{4}$$

K_F is the radiative rate constant, τ_R is the radiative lifetime, n_f and n_a are the refractive indices of the medium at the mean frequency of the emission and the absorption respectively, $\epsilon(\nu)$ is the extinction coefficient at frequency ν and $I(\nu)$ is the fluorescence intensity at frequency ν. For eqn. (3) to be applicable it is necessary that the singlet–singlet transition be allowed (say $\epsilon_{max} > 8000$ dm^3 mol^{-1} cm^{-1}) and that there is no large change in the nuclear configuration between the ground and the excited singlet states [33]. A further requirement is that only the relevant absorption band is included in the range over which $\int \epsilon(\nu)\, d\nu/\nu$ is calculated. Equation (3), however, has been shown to apply almost exactly to the fluorescence decay of DPA in a non-polar solvent [34].

Various theories have been developed which lead us to expect that the value of $\epsilon(\nu)$ will show some dependence on the refractive index of the medium. However, the calculated dependences are different for the various theoretical models. For example, Birks [35] calculates an n dependence, whereas Bakhshiev *et al.* [30] find the dependence to be $9n^3/(2n^2 + 1)$. Chako [31] assembled a substantial body of data on this problem and proposed a different correction, but he did not find the observed medium effects on $\epsilon(\nu)$ to be predictable on the basis of any one theoretical model; the refractive index correction appeared to show some dependence on the nature of the chromophore. The various refractive index corrections, which may apply to the value of $\epsilon(\nu)$, have been collected in ref. 36.

The oscillator strengths of DPA in some non-polar solvents have been calculated previously [26] and have been found to be constant, regardless of the solvent refractive index; it was aptly pointed out that each of the derived correction factors may be more or less valid, and that they may cancel each other out (see Tables 1 and 2 or ref. 36). As a consequence of this we can consider the value of the extinction coefficient required in eqn. (3) to be essentially independent of the medium for DPA.

The value of $\langle \bar{\nu}_f^{-3} \rangle_{AV}^{-1}$ will show some dependence on the shape and the position of the fluorescence spectrum. We have calculated the solvent dependence of this parameter using eqn. (4) and the results are shown in Table 5 together with the frequency of the absorption and emission maxima and the Stokes shift. The solvent dependence of the absorption and emission spectra are shown in Figs. 2 and 3. In both cases there is a small shift to a lower energy as the refractive index of the solvent increases. No change, within the experimental error, is observed in the value of the Stokes shift. In all solvents the shapes of the spectra are independent of the solvent. The value of $\langle \bar{\nu}_f^{-3} \rangle_{AV}^{-1}$ increases slightly, but consistently, as the refractive index of the medium increases (*i.e.* as the spectrum shifts to lower energies).

The data in Table 5 provide no evidence for a strong or anomalous solvent effect on DPA which might enhance either the radiative or non-radia-

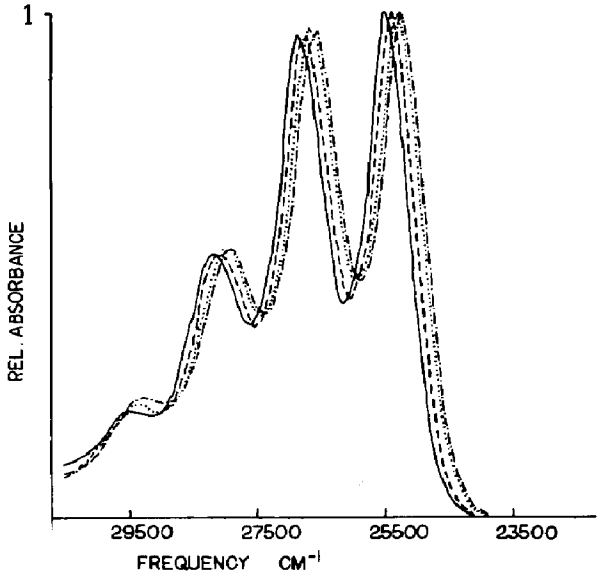

Fig. 2. Absorption spectra of DPA in hexane (——), cyclohexane (— — —), decalin (·····), and benzene (— · —).

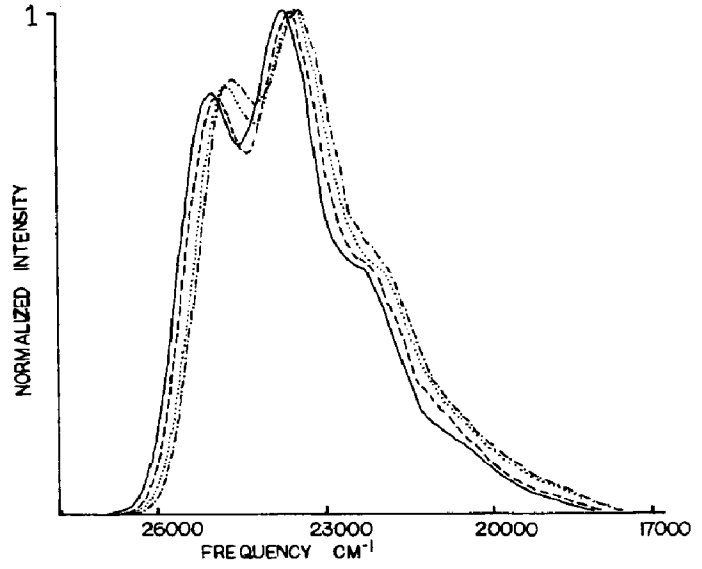

Fig. 3. Emission spectra of DPA in hexane (——), cyclohexane (— — —), decalin (·····) and benzene (— · —).

tive processes. The small spectral shifts observed do not seem large enough to cause any significant change in k_{nr}.

It can easily be shown that the use of n_D^2 in eqn. (3), where n_D is the value of n at the sodium D line, rather than n_f^3/n_a does not lead to a serious error.

To allow the comparison of radiative lifetimes obtained in different solvents or at different temperatures, a correction clearly has to be applied for the refractive index of the medium, as can be seen from eqn. (3); such corrections have only rarely been made. However, when accurate quantum yields and lifetimes are available, and solution and gas phase results are being compared or quite small solvent-dependent changes in k_f are being sought, some correction should be made. Unfortunately the precise correction has been the subject of some dispute. Birks [35] has proposed an n^2 correction. Olmsted [37], in a study of the temperature dependence of the fluorescence lifetime of DPA in cyclohexane in which both k_f and k_{nr} were assumed to be temperature independent, was unable to distinguish between an n^2 and an n^3 correction.

In Table 6 we present values of τ_R corrected by factors of unity, n, n^2 and n^3. The values of τ_R calculated in an identical way with the assumption that the yield of DPA is solvent independent and equal to 0.93 are presented in Table 7. These data are plotted in Fig. 4. On this basis, if our assumption of a radiative lifetime which is independent of the medium is valid, we can rule out as inapplicable the unity and n^3 corrections; n^2 gives the best results, but n is also quite close. However, a comparison of the data obtained in the solution and vapour phases [36] seems to rule out n. Thus we conclude that an n^2 correction should be applied to radiative lifetime measurements in solution.

Interestingly, this relationship allows us to re-evaluate the data of Morris *et al.* (ref. 26, Table 1). They conclude, also on the basis of a medium-independent radiative lifetime, that the solvent-dependent quantum yields which they had measured in the absence of a geometrical refractive index correction were correct. Those quantum yields to which an n^2 geometrical correction had been applied were independent of the solvent, as is found (to a good approximation) here using the integrating sphere method. If, however, the theoretical n^2 correction is considered and applied to the results of ref. 26, then the reverse of their conclusion is true and the solvent-independent values of ϕ_F give the constant radiative lifetime predicted. This implies that the geometrical n^2 refractive index correction is valid, at least under the conditions stated in ref. 26.

TABLE 6

Refractive index dependence of the radiative lifetime of 9,10-diphenylanthracene in non-polar solvents (using ϕ_F data from Table 4)

Solvent	n	τ_R (ns)	$n\tau_R$ (ns)	$n^2\tau_R$ (ns)	$n^3\tau_R$ (ns)
Hexane	1.375	8.867	12.19	16.767	23.058
Cyclohexane	1.426	8.412	11.99	17.101	24.384
Decalin	1.473	7.628	11.24	16.552	24.384
Benzene	1.501	7.476	11.22	16.844	25.282

TABLE 7

Refractive index dependence of the radiative lifetime of 9,10-diphenylanthracene in non-polar solvents (ϕ_F constant and equal to 0.93)

Solvent	τ_R (ns)	$n\tau_R$ (ns)	$n^2\tau_R$ (ns)	$n^3\tau_R$ (ns)
Hexane	8.608	11.837	16.278	22.384
Cyclohexane	8.285	11.813	16.843	24.02
Decalin	7.735	11.394	16.785	24.728
Benzene	7.702	11.561	17.352	26.047
Ethanol[a]	8.84	12.11	16.59	22.731

[a] τ_F was obtained from ref. 26; n = 1.37.

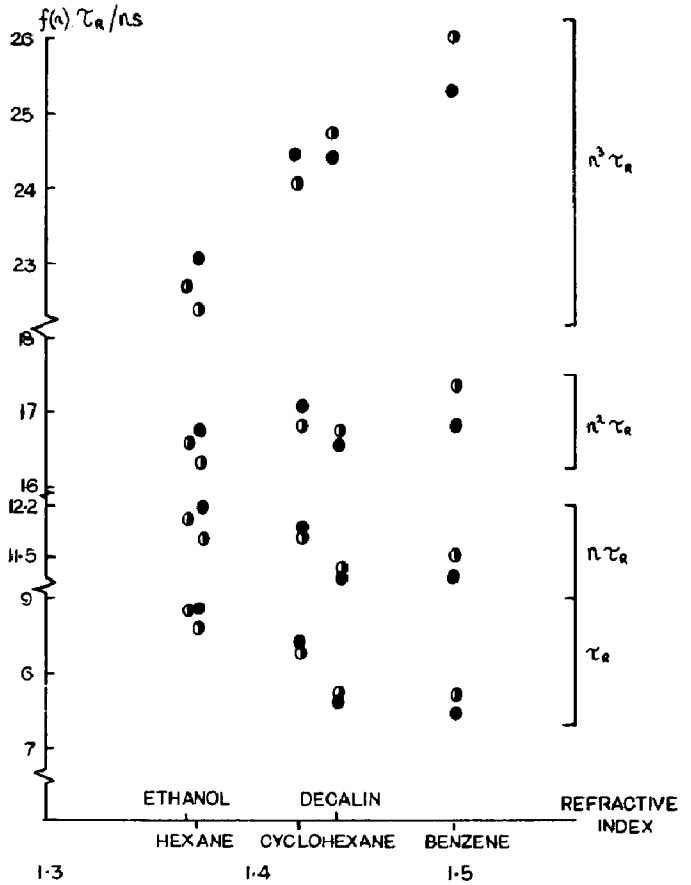

Fig. 4. $f(n)\tau_R$ measured (●) (*i.e.* data from Table 6) or calculated (◑) assuming that ϕ_F(DPA) = 0.93 in all solvents.

Consequently this yields an independent confirmation that the quantum yield of DPA in non-polar solvents is essentially constant. Hence the expected constancy of the ratio of ϕ_F(QBS–1 N H_2SO_4) to ϕ_F(DPA–non-polar solvent) can be used to determine an empirical value of the geometrical

refractive index correction for fluorometers of any viewing geometry. However, the data of ref. 26 as discussed above suggest that the n^2 geometrical correction is not seriously in error, which is in accord with recent theoretical predictions [15 - 17].

3.3. Quinine bisulphate in H_2SO_4 solutions

We have recently reported the complex wavelength-dependent fluorescence decay kinetics of this rather widely used fluorescence standard [8]. Here we wish to discuss our measurements of the temperature and acid concentration dependence of the non-exponential fluorescence decay and to outline a model which accounts for both our observations and the previously reported complex spectral behaviour of this molecule [38].

We can summarize our previous observations made at room temperature in 1 N H_2SO_4 as follows. The fluorescence decay of QBS is both non-exponential and wavelength dependent. A good fit to a single exponential is not obtained at any wavelength. On the blue edge (400 - 450 nm) of the emission we observe two decaying components. First a minor (about 2%) short-lived (about 2.5 ns) component is found, the amplitude of which increases as the analysing wavelength is moved further into the blue edge of the emission. The second longer-lived (19 - 20 ns) decay is the major component and is very similar to, or slightly shorter than, the single-exponential lifetime usually measured (see below). On the red edge of the emission (500 - 575 nm) a short component (about 2 ns) with a negative pre-exponential factor (a rise time) is observed together with a dominant (about 20.5 ns) decaying component. Time-resolved emission spectroscopy [8] reveals that the short-lived component is blue shifted compared with the longer-lived component.

The QBS fluorescence decay at 425 and 525 nm in four acid solutions is shown in Tables 8 and 9 fitted to single-exponential and double-exponential decay functions respectively. The decay is non-exponential in all samples and a rise time on the red edge is observed. It can be seen that the short lifetime (425 nm) is essentially independent of acid concentration. The rise time (525 nm) is quite close to the fast decay time at 425 nm, but the problems associated with determining short decay times, particularly distortions due to photomultiplier tube effects [13], do not allow us to state that the two processes are related. We cannot even be certain that each is described by a single rate constant. We have attempted to use a shift routine to correct for photomultiplier tube distortions, in which case the relationship between the two processes is greatly improved (Tables 8 and 9), but such corrections are notoriously unreliable when a fast rise time exists in the decay profile.

The long decay time, which represents the major portion of the emission, reduces as the concentration of the acid decreases. This decrease reflects quite accurately the observed decrease in the measured quantum yield [23]. The long decay on the blue edge was slightly, but significantly, shorter than that on the red edge. The ratio of τ_{long}^{425} to τ_{long}^{525} is independent of the acid concentration. This suggests that the mechanism which acts

TABLE 8

Emission at 425 and 525 nm from quinine bisulphate in various acids at 20 °C fitted to a single-exponential function

Acid concentration (N)	λ (nm)	A	τ [a]	χ_ν^2 [b]	D [c]
3.6	425	1.44	19.75 (0.02)	7.5	0.30
	525	1.78	21.85 (0.003)	2.1	0.91
1.8	425	1.55	19.10 (0.02)	7.4	0.26
	525	1.94	21.00 (0.003)	1.6	1.20
1.0	425	1.48	19.02 (0.003)	8.8	0.23
	525	1.80	20.85 (0.001)	2.6	0.98
0.1	425	1.49	17.93 (0.01)	8.0	0.24
	525	1.84	19.88 (0.02)	2.6	0.78

[a] The numbers in parentheses represent the standard deviations.
[b] $1 < \chi_\nu^2 < 1.2$ implies a good fit.
[c] Durbin–Watson parameter [13]. $D > 1.65$ implies a good fit for a single-exponential function.

TABLE 9

Emission at 425 and 525 nm from quinine bisulphate in various acids at 20 °C fitted to a double-exponential function

Acid concentration (N)	*Analysis* λ (nm)	A_1	τ_1 [a]	A_2	τ_2 [a]	χ_ν^2	D [b]	$\tau_{long}^{425}/\tau_{long}^{525}$ [c]
3.6	425	0.34	2.63 (0.09)	1.36	20.43 (0.03)	0.99	1.98	
	525	−0.22	2.02 (0.19)	1.81	21.63 (0.02)	1.02	1.79	0.94
	WC + S [d]	−0.19	2.33 (0.13)	1.81	21.61 (0.02)	1.03	1.77	
1.8	425	0.38	2.65 (0.12)	1.46	19.76 (0.03)	1.00	1.93	
	525	−0.25	2.18 (0.26)	1.97	20.82 (0.02)	1.02	1.96	0.95
	WC + S [d]	−0.19	2.6 (0.24)	1.93	21.07 (0.03)	1.4	1.61	
1.0	425	0.36	2.59 (0.09)	1.39	19.74 (0.03)	1.1	1.87	
	525	−0.23	2.28 (0.19)	1.83	20.59 (0.03)	1.23	2.04	0.96
	WC + S [d]	−0.19	2.77 (0.16)	1.83	20.57 (0.03)	1.27	1.98	
0.1	425	0.38	2.63 (0.09)	1.40	18.59 (0.04)	1.04	1.83	
	525	−0.22	2.12 (0.16)	1.88	19.63 (0.02)	1.1	1.84	0.95
	WC + S [d]	−1.1	0.27 (0.01)	1.85	19.85 (0.02)	2.5	—	

[a] The numbers in parentheses represent the standard deviations.
[b] Durbin–Watson parameter. $D > 1.75$ implies a good fit for a double-exponential function.
[c] See text.
[d] WC + S implies that the decay was analysed over all the data points (whole curve) and a shifting routine was employed to correct for the wavelength dependence of the photomultiplier tube.

TABLE 10

Decay characteristics of quinine bisulphate in 1.0 N H_2SO_4 solution: temperature dependence at 415 and 500 nm fitted to a double-exponential decay function

T (°C)	λ (nm)	A_1	τ_1 [a] (ns)	A_2	τ_2 [a] (ns)	χ_ν^2
20	415	0.27	2.37 (0.04)	1.01	19.53 (0.02)	1.2
	500	−0.08	1.91 (0.3)	1.82	20.67 (0.02)	1.2
40	415	0.23	1.68 (0.04)	1.05	18.47 (0.02)	1.3
	500	−1.63	0.09	1.77	19.87 (0.02)	1.2
59	415	0.21	1.33 (0.04)	1.07	17.19 (0.02)	1.3
	500	−1.46	0.07	1.65	19.11 (0.02)	1.2
71	415	0.17	1.54 (0.04)	1.12	16.32 (0.02)	1.6
	500	−1.60	0.6	1.73	18.76 (0.02)	1.4

[a]The numbers in parentheses represent the standard deviation.

to reduce the quantum yield affects both of these lifetimes equally: some non-radiative process is clearly suppressed by the acid.

The difference between the lifetimes at the two wavelengths is, from the experimental errors, significant. We do not believe that this small difference is another wavelength-dependent artefact since we have not observed such changes for other (exponentially decaying) systems such as DPA or 2AP. Also the major change in the magnitude of the long lifetime occurs between 425 and 500 nm, and it is essentially constant between 500 and 575 nm. Consequently we believe the observed change to be real.

We have also studied the temperature dependence of the fluorescence decay of QBS in aqueous H_2SO_4. The two-component fits to the temperature-dependent decay at 415 and 500 nm are shown in Table 10. The one-component fit to the 500 nm data is shown in Table 11, and the two-component fit to the decay at 425 and 525 nm at 76 °C only is shown in Table 12 for two acid concentrations.

The temperature dependence is surprising. It is immediately noticeable that the rise time on the red edge is absent, or at least immeasurably small, at all the temperatures studied above 20 °C. Comparison of Tables 10 and 11 suggests that the decay at 500 nm is reasonably well described by a single-exponential function at temperatures above 20 °C. The fits to these data are not very good, but this is almost certainly due to the previously mentioned photomultiplier tube effects since all these data are analysed over the whole of the decay profile without using the shift. This is probably the origin of the very short lifetimes recovered in the double-exponential analysis [13].

The double-exponential character of the blue edge is retained at all temperatures; these data are not well described by a single-exponential function. In the 1 N H_2SO_4 solution the short decay time decreases with increasing temperature; this is not observed for the other acid concentrations (Table 12) but these latter results have rather large errors. We conclude that the

TABLE 11

Decay characteristics of quinine bisulphate in 1 N H_2SO_4 solution: temperature dependence at 500 nm fitted to a single-exponential function

T (°C)	τ (ns)	χ_ν^2
20	20.68	1.5
40	19.87	1.2
59	19.11	1.2
71	18.77	1.4

TABLE 12

Fluorescence decay of quinine bisulphate in two acid solutions at 76 °C fitted to a double-exponential function

Solvent	λ (nm)	A_1	τ_1 [a] (ns)	A_2	τ_2 [a] (nm)	χ_ν^2
Aqueous 3.6 N H_2SO_4	425	0.17	4.25 (0.27)	1.41	17.83 (0.03)	1.2
	525	−0.48	0.28 (0.02)	1.83	19.91 (0.03)	1.3
Aqueous 0.1 N H_2SO_4	425	0.21	2.52 (0.16)	1.51	15.45 (0.02)	1.2
	525	−0.91	0.14 (0.04)	1.58	18.50 (0.10)	1.3

[a]The numbers in parentheses represent the standard deviation.

short decay time on the blue edge, which is independent of acid concentration, is probably temperature dependent as it reduces by about 35% between 20 and 71 °C.

The wavelength dependence of the longer lifetime as a function of the temperature is interesting. For changes in the acid concentration (Table 9), where the long lifetime changed over the whole acid range by about 10%, the ratio $\tau_{long}^{425}/\tau_{long}^{525}$ was constant (0.95 ± 0.1). However, as we increase the temperature of the 1.0 N solution from 20 to 71 °C, causing a total change in the lifetime of about 9% - 15% (depending on the wavelength), the ratio $\tau_{long}^{415}/\tau_{long}^{500}$ changes from 0.94 to 0.87. (This is in reasonable agreement with the observation that the temperature dependence of the quantum yield is about −0.25% $°C^{-1}$ [21].) This suggests that the decrease in the quantum yield with decrease in the acid normality quenches the quinoline fluorophore, but that the temperature effect on the wavelength dependence and the quantum yield is indirect. Consequently the wavelength and temperature dependence must be considered separately from the acid dependence.

The above represents a comprehensive collection of data on the decay of QBS in H_2SO_4 solutions. A plausible mechanism, which is consistent with the observed complex kinetics and with other features of the spectroscopy of the QBS–H_2SO_4 system, is outlined below.

The data have been analysed in terms of a dual-exponential decay function because they do not justify the use of a more complex expression. However, a two-state model (*e.g.* a short-lived state decaying radiatively and simultaneously populating the longer state) is not consistent with our results. Both the wavelength dependence of the long decay time (increasing from about 19.8 to 20.6 ns between 425 and 525 nm) and the failure to relate conclusively the fast decay on the blue edge to the 525 nm rise time argue against a two-state model. Thus a multiple-state model is required to account for the above observations. The results are explicable in terms of a range of states, centred about two major states, which can plausibly be ascribed to different conformations of the side chain existing in the ground state.

The temperature dependence of the fluorescence decay would suggest that at least some of the conformations that have short excited state lifetimes are somewhat isolated from the other states, whereas some may interconvert freely with the longer-lived conformations to yield a rise time (at 20 °C). This conclusion arises from a study of the temperature dependence (Table 10), because the short decay time (which arises from a blue-shifted species [8]) is observed at higher temperatures whereas the red edge rise time is not (or is not resolved as separating rapid rise times from fluorescence decays can be difficult [39]). Thus the red edge rise time may be due to less stable ground state conformations. The temperature dependence of $\tau_{long}^{425}/\tau_{long}^{525}$ also supports this qualitative model; a diagrammatic representation is given in Fig. 5.

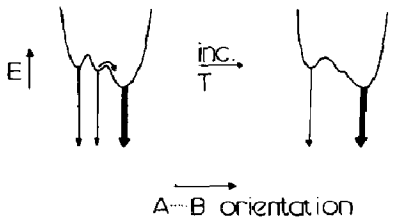

Fig. 5. Postulated potential energy surfaces along the quinoline–quinuclidine coordinate. The thickness of the lines indicates the relative importance of the process.

It should be noted that this model predicts the edge excitation red shift (EERS) that is observed for QBS in 1 N H_2SO_4 [38]. It is noteworthy that the type of non-exponential decay and red edge rise time observed here is also observed for other systems exhibiting EERS such as aminonaphthalenes in viscous alcohols [40, 41]. These effects have been ascribed to different (non-specific) solvent–solute configurations existing on a time scale longer than the fluorescence decay [42]. However, a model emphasizing the role of side chain conformation in these complex decay kinetics is preferable, since other systems, which exhibit the effects of non-specific solvent–solute interactions in aqueous solutions more markedly than does QBS, decay exponentially [40]. However, a role for the medium in the observed complexities of QBS fluorescence cannot be ruled out at this stage.

The reason for the very rapid decay (which is presumably mainly radiationless) of the isolated short-lived state is not known. It could, however, be associated with the fact that quinoline itself has a very marked dependence of quantum yield on the medium [43]. Possibly the medium is sufficiently perturbed by the conformation changes to facilitate a rapid radiationless relaxation.

The dependence of ϕ_F on the acid concentration is not included in this model and does appear to be a separate problem (see above). Quinine fluorescence is in fact quenched by SO_4^{2-} when the acid concentration is somewhat lower than that employed here [23], *i.e.* the plot of ϕ_F against $[H_2SO_4]$ passes through a minimum. Since it is unlikely that quinine can exist in two chemically distinct forms (*e.g.* sulphate and bisulphate) at these high acid and low sample concentrations, it seems more likely that the variation in ϕ_F is due to an effect of acid concentration on the structure of the medium surrounding the quinine molecule. This could conceivably lead to the suppression of some non-radiative channel.

In conclusion, we have observed a rather complex dependence of the non-exponential decay of QBS in aqueous H_2SO_4 solutions on both the temperature and the wavelength of emission of the system. The kinetic data presented and other spectral data [38] can be adequately accounted for by a distribution of chromophore–side chain conformations. There are at least two, and probably more, stable conformations in the excited state. The distribution is dependent on both the temperature and whether the chromophore is in the ground or first excited singlet state. Some of the conformations may interconvert, and each conformation has its own particular non-radiative rate.

The role of the medium, the mechanism of the non-radiative decay and several other points are still unclear. Further work on these problems is in progress.

3.4. 2-aminopyridine in H_2SO_4 solutions

2AP has many of the properties which make QBS such a good quantum yield standard, *i.e.* high yield, unstructured absorption and emission spectra with only a small overlap, ease of purification and wavelength-independent yield. The last point was determined from lifetime measurements. It was by using this "quantum counting" property that we were able to confirm the unsuitability of RB as a quantum counter [19]. 2AP can be regarded as a complementary standard to QBS, since it has a relatively strong absorption in the QBS window and its emission is blue shifted compared with that of QBS. Its standard spectrum can be used to correct luminescence detection systems [18].

Unfortunately there is some disagreement on the value of the quantum yield. We measured values of 0.65 (±0.04) and 0.66 (±0.05) for 2AP in 1 N H_2SO_4 and 0.1 N H_2SO_4 solutions respectively (Tables 1 and 2) relative to $\phi_F = 0.546$ for QBS in 1 N H_2SO_4. The excitation wavelengths were between 280 and 315 nm. Chen [23] found, for 0.1 N acid solutions, $\phi_F = 0.73$ rela-

TABLE 13

The temperature dependence of the fluorescence decay characteristics of 2-aminopyridine in 1 N H_2SO_4

T (K)	ϕ_F calc [a]	τ_F [b] (ns)	$\sum_n k_{nr}$ (s)	$\phi_F^{-1} - 1$
293	0.65[b]	9.66	3.62	0.539
312	0.59	8.81	4.62	0.695
321	0.55	8.20	5.47	0.818
334	0.48	7.09	7.37	1.083
341	0.43	6.42	8.84	1.326
349	0.40	5.88	10.30	1.500

[a] See text.
[b] Measured value (see Table 1).

tive to DPA in cyclohexane ($\phi_F = 1.00$), tryptophan in water ($\phi_F = 0.12$) and QBS in 1 N H_2SO_4 ($\phi_F = 0.55$). Rustakowicz and Testa [25] reported the yield of 2AP in 0.1 N H_2SO_4 as 0.60 (±0.06) relative to QBS in 0.1 N H_2SO_4 ($\phi_F = 0.46$) and DPA in cyclohexane ($\phi_F = 1.00$); the excitation wavelength was 285 nm. This result was later re-evaluated as 0.64 [44]. There is, to our knowledge, no absolute measurement of this quantum yield. Such a measurement is required. There is a similar spread in the measured values of τ_F. We find $\tau_F = 9.6$ ns, independent of acid concentration and excitation wavelength, but values of 11.2 ns [44] and 12.7 ns [23] have been reported.

While this system is clearly not as well characterized as QBS, it does have gratifyingly simpler decay kinetics. We did not observe any EERS effects. The fluorescence decay is monoexponential and independent of the excitation and emission wavelengths used. The only unusual feature observed is a relatively strong temperature dependence of the non-radiative decay. Table 13 shows that τ_F decreases by about 40% between 20 and 76 °C.

For any one excited electronic state

$$\tau_F = \frac{1}{K_F + \sum_n k_{nr}} \tag{5}$$

and

$$\phi_F = \frac{K_F}{K_F + \sum_n k_{nr}} \tag{6}$$

where K_F is the radiative rate constant and k_{nr} represents the non-radiative processes. If we make the usually valid assumption that the radiative rate K_F is independent of the temperature, then we can calculate the temperature

dependence of the fluorescence quantum yield, the parameter of interest, from the following well-known relation derived from eqns. (5) and (6):

$$\phi_F^{T\,K} = K_F^{293\,K} \tau_F^{T\,K} \tag{7}$$

where K_F has been calculated from the measured quantum yield and the lifetime at 293 K ($K_F^{293\,K} = 6.73 \times 10^7\ s^{-1}$) and superscripts refer to temperature T in kelvins. By using eqns. (6) and (7) and assuming the value of K_F, we can calculate the magnitude of the non-radiative rate constants from

$$\sum_n k_{nr}^{T\,K} = \frac{1}{\tau_F^{T\,K}} - K_F^{293\,K} \tag{8}$$

These data are shown in Table 13.

Equation (6) can also be rewritten as follows to include explicitly the temperature dependence of the non-radiative rates:

$$\frac{1}{\phi_F^{T\,K}} - 1 = \frac{1}{K_F^{293\,K}} \sum_n A_n \exp\left(-\frac{E_a}{RT}\right) \tag{9}$$

where E_a is the activation energy of the nth non-radiative process, the pre-exponential factor A_n is its amplitude, R is the gas constant and T is the temperature in kelvins. If only one non-radiative rate is important then eqn. (9) reduces to

$$\frac{1}{\phi_F^{T\,K}} - 1 = \frac{A_0}{K_F^{293\,K}} \exp\left(-\frac{E_a}{RT}\right) \tag{10}$$

in which case a plot of $\ln(1/\phi_F^{T\,K} - 1)$ against $1/T$ should be linear and the slope will yield the activation energy E_a directly. Such an analysis is presented in Fig. 6. The calculated activation energy is 4.783 kcal mol^{-1}

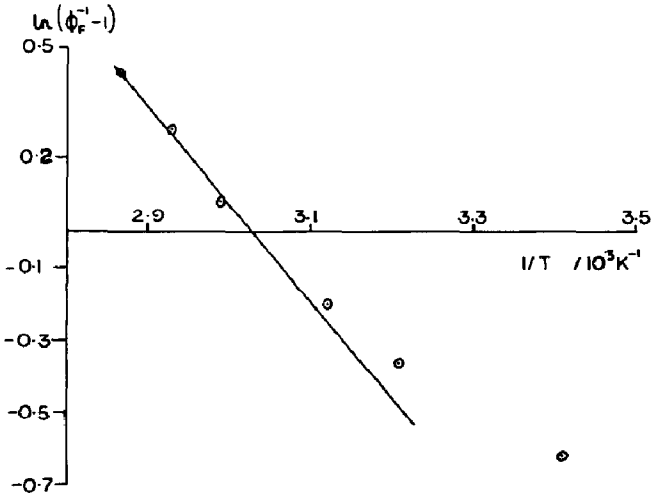

Fig. 6. Analysis of the temperature dependence of 2AP fluorescence according to eqn. (10).

(0.207 eV); however, the linearity of the plot is not good as curvature occurs in the low temperature region. Consequently we conclude that the assumed behaviour implicit in eqn. (10) does not describe the true decay processes of the excited state of 2AP.

Kirby and Steiner [45] have presented data for the temperature dependence of indole fluorescence in aqueous solution in which a similar deviation was observed. A more complex analysis of our data is, given the small deviation, rather difficult. However, one possible situation, other than that just described, can be analysed, *i.e.* the single temperature-dependent and single temperature-independent radiationless deactivation processes. When the second method of analysis given in ref. 45 is used (a similar method was proposed by Walker *et al.* [46]), eqn. (9) can be written as

$$\frac{1}{\phi_F{}^{T\,K}} - 1 = \frac{A_0}{K_F{}^{293\,K}} + \frac{A_T}{K_F{}^{293\,K}} \exp\left(-\frac{E_a}{RT}\right) \tag{11}$$

or

$$\ln\left(\frac{1}{\phi_F{}^{T\,K}} - 1\right) - \frac{A_0}{K_F{}^{293\,K}} = \ln\left(\frac{A_T}{K_F{}^{293\,K}}\right) - \frac{E_a}{RT} \tag{12}$$

where A_0 and A_T are the amplitudes of the temperature-independent and temperature-dependent processes respectively and have units of reciprocal seconds. It is now a simple matter to select empirically the value of $A_0/K_F{}^{293\,K}$ which gives the best straight line fit to a plot of the left-hand side of eqn. (12) against $1/T$. We present this analysis in Fig. 7 for $A_0/K_F{}^{293\,K} = 0.4$; clearly the linearity is greatly improved. The activation energy thus obtained

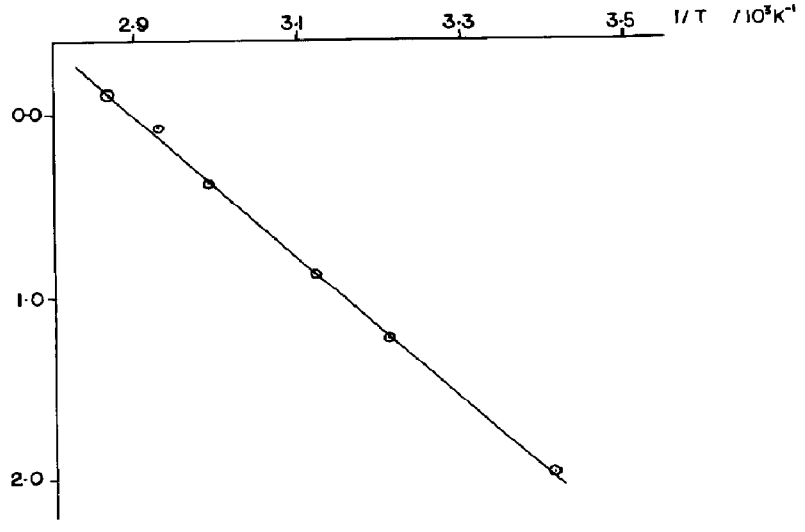

Fig. 7. Analysis of the temperature dependence of 2AP fluorescence according to eqn. (12).

is 7.690 kcal mol^{-1} (0.336 eV). We should note here that this analysis is rather approximate and cannot, for instance, distinguish between the assumed two radiationless de-excitation processes and more complex situations. Also, quite large errors may occur in the derived parameters.

We can calculate from the data derived above and from Fig. 7 and Table 13 that at 20 °C 65% of the excited state depletion is by fluorescence, 26% by the temperature-independent process and 9% by the temperature-dependent process. The corresponding values for 76 °C are 40%, 16% and 44% respectively. Thus the temperature dependence of the quantum yield of 2AP in 1 N H_2SO_4 (about 0.7% $°C^{-1}$ (the relationship is not linear)) is almost three times that of QBS. This must be borne in mind if 2AP is to be used as a quantum yield or lifetime standard.

The origin of the two postulated non-radiative processes is not clear. A probable candidate for the temperature-independent process is intersystem crossing to the lower triplet states. Three triplet states are found by complete neglect of differential overlap calculations [44] to lie between S_1 and S_0. Thermally activated intersystem crossing would seem to be ruled out for the temperature-dependent process owing to the large energy gap between S_1 and the next-highest triplet state ($\Delta E(S_1-T_4) \approx 0.75$ eV). Photoejection of electrons appears to be quite a common fate of heteroaromatic systems in aqueous media. The activation energy for such a process will vary somewhat from system to system and will probably depend on the nature of the trap formed by the water molecules, which may in turn depend on the nature of the molecule. Obviously, more work is required before we can assign the radiationless process(es) to particular mechanisms.

Coupling of the fluorescent state to higher-lying n,π^* states may also be important. This question may be resolved by transient absorption measurements.

In summary, 2AP in H_2SO_4 solution exhibits a much simpler photophysical behaviour than QBS and also shows many of its desirable properties as a standard. However, there is still considerable disagreement about the value of the quantum yield; our own careful measurement gives $\phi_F = 0.66 \pm 0.05$. For this reason 2AP must be considered as a secondary standard to QBS, except for the fact that it absorbs in the window region of QBS. Further independent observations of the fluorescence lifetime are required before it can be used as a standard for calibrating time-resolved instruments. The rather strong and quite complex temperature dependence should be remembered if 2AP is to be used as an acceptable quantum yield standard.

4. Conclusion

We have found a complex fluorescence decay for QBS in H_2SO_4 solutions which can be tentatively assigned to various conformers leading to various interactions between the main chromophore and the side chain. If this finding is correct then the fluorescence decay of this system cannot be

used to calibrate time-resolved spectrometers. This does not affect the steady state behaviour, and we have been able to repeat all the previous observations in the literature which have made this such a good system for the measurement of relative quantum yields; QBS in 1 N H_2SO_4 must still be considered the primary fluorescence standard for such measurements.

2AP in H_2SO_4 solutions has a much simpler lifetime behaviour than QBS, although there is a rather strong dependence on temperature. This system also exhibits many of the useful features found in the QBS system, and hence 2AP is a potentially good fluorescence standard for both lifetime and quantum yield measurements. Unfortunately there is some disagreement about the absolute values of these parameters. Further work on this system is desirable.

We have found that DPA has a constant quantum yield in four different non-polar solvents; a similar result can be inferred from previous measurements [26]. This result allows an empirical determination to be made of the geometrical refractive index correction for individual spectrofluorometers. We have also found that, if the assumptions outlined in Section 3.2 are valid, then an n^2 theoretical correction is required for the radiative lifetime of a molecule measured in media of differing refractive indices. The quantum yield of a dilute solution of DPA in cyclohexane is independent of the excitation wavelength over the first absorption band and is almost independent over the second absorption band. However, the appreciable structure in the absorption spectrum and the need for rigorous degassing suggests that this system is not an ideal quantum yield standard. The fluorescence decay of dilute solutions of DPA in non-polar solvents invariably gave a good fit to a single-exponential function, and the scatter of various lifetimes obtained, both here and in the literature (Tables 3 - 5), is quite small. Thus this may be an ideal standard for calibrating time-resolved spectrofluorometers.

References

1 J. B. Birks (ed.), *Excited States of Biological Molecules*, Wiley, New York, 1978.
2 A. J. Roberts, D. V. O'Connor and D. Phillips, *Ann. N.Y. Acad. Sci.*, *366* (1981) 109.
3 J. Darwent, P. Douglas, A. Harriman, G. Porter and M.-C. Richoux, *Coord. Chem. Rev.*, *44* (1982) 83.
4 G. R. Fleming, *Adv. Chem. Phys.*, *49* (1982) 1.
5 J. N. Demas and G. A. Crosby, *J. Phys. Chem.*, *75* (1971) 991.
6 C. A. Parker and W. T. Rees, *Analyst (London)*, *85* (1960) 587.
7 C. A. Parker, *Photoluminescence of Solutions*, Elsevier, Amsterdam, 1968.
8 D. V. O'Connor, S. R. Meech and D. Phillips, *Chem. Phys. Lett.*, *88* (1982) 22.
9 S. I. Vavilov, *Z. Phys.*, *42* (1927) 311.
10 G. Weber and F. W. J. Teale, *Trans. Faraday Soc.*, *53* (1957) 646.
11 W. R. Dawson and M. W. Windor, *J. Phys. Chem.*, *72* (1968) 3251.
12 G. A. Crosby, J. N. Demas and P. Callis, *J. Res. Natl. Bur. Stand., Sect. A*, *76* (1972) 561.
13 R. A. Lampert, L. A. Chewter, A. J. Roberts, D. Phillips, D. V. O'Connor and S. R. Meech, *Anal. Chem.*, *55* (1983) 68.

14 J. J. Hermans and S. Levinson, *J. Opt. Soc. Am.*, *41* (1950) 460.
15 F. J. Buselle, N. D. Haig and C. Lewis, *Chem. Phys. Lett.*, *72* (1980) 583.
16 M. D. Ediger, R. A. Moog, S. G. Boxer and M. D. Fayer, *Chem. Phys. Lett.*, *88* (1982) 123.
17 F. J. Buselle, N. D. Haig and C. Lewis, *Chem. Phys. Lett.*, *88* (1982) 127.
18 W. H. Melhuish, *J. Res. Natl. Bur. Stand., Sect. A*, *76* (1972) 547.
19 W. H. Melhuish, *Appl. Opt.*, *14* (1975) 26.
20 S. R. Meech, *Ph.D. Thesis*, University of Southampton, 1983.
21 W. H. Melhuish, *J. Phys. Chem.*, *65* (1961) 229.
22 B. Gelerent, A. Findeisen, A. Stein and J. A. Poole, *J. Chem. Soc., Faraday Trans. II*, *70* (1973) 939.
23 R. F. Chen, *J. Res. Natl. Bur. Stand., Sect. A*, *76* (1972) 593.
24 G. Heinrich, S. Schoof and H. Gusten, *J. Photochem.*, *3* (1975) 315.
25 R. Rustakowicz and A. C. Testa, *J. Phys. Chem.*, *72* (1968) 2680.
26 J. V. Morris, M. A. Mahaney and J. R. Huber, *J. Phys. Chem.*, *80* (1976) 969.
27 S. Hamai and F. Hirayama, *J. Phys. Chem.*, *87* (1) (1983) 83.
28 D. J. S. Birch and R. E. Imhof, *Chem. Phys. Lett.*, *32* (1975) 56.
29 D. J. S. Birch, personal communication, 1981.
30 N. G. Bakhshiev, O. P. Girin and V. S. Libov, *Opt. Spectrosc. (U.S.S.R.)*, *23* (1967) 16, 124.
31 N. Q. Chako, *J. Chem. Phys.*, *2* (1934) 644.
32 W. R. Ware and W. Rothman, *Chem. Phys. Lett.*, *39* (1976) 449.
33 S. J. Strickler and R. A. Berg, *J. Chem. Phys.*, *37* (1962) 814.
34 J. B. Birks and J. D. Dyson, *Proc. R. Soc. London, Ser. A*, *275* (1963) 135.
35 J. B. Birks, *Photophysics of Aromatic Molecules*, Wiley-Interscience, New York, 1970.
36 S. Hirayama and D. Phillips, *J. Photochem.*, *12* (1980) 139.
37 J. Olmsted III, *Chem. Phys. Lett.*, *38* (1976) 287.
38 A. N. Fletcher, *J. Phys. Chem.*, *72* (1968) 2742.
39 A. Gafni, R. P. De Toma, R. E. Manrow and L. Brand, *Biophys. J.*, *17* (1977) 155.
40 S. R. Meech, D. V. O'Connor, D. Phillips and A. G. Lee, *J. Chem. Soc., Faraday Trans. II*, to be published.
41 B. Valeur and G. Weber, *J. Chem. Phys.*, *69* (1978) 2393.
42 K. I. Itoh and T. Azumi, *J. Chem. Phys.*, *62* (1975) 3431.
43 T.-I. Lai and E. C. Lim, *Chem. Phys. Lett.*, *65* (1979) 507.
44 A. C. Testa and U. P. Wild, *J. Phys. Chem.*, *85* (1981) 2367.
45 E. P. Kirby and R. F. Steiner, *J. Phys. Chem.*, *74* (1970) 4480.
46 M. S. Walker, T. W. Bednar, R. Lumry and F. Humphries, *Photochem. Photobiol.*, *14* (1971) 147.